IJC
International Journal of Cancer

Next-generation sequencing reveals a novel role of lysine-specific demethylase 1 in adhesion of rhabdomyosarcoma cells

Tinka Haydn[1], Sarah Kehr[1], Dominica Willmann[2], Eric Metzger[2], Roland Schüle[2] and Simone Fulda[1,3,4]

[1]Institute for Experimental Cancer Research in Pediatrics, Goethe-University Frankfurt, Frankfurt, Germany
[2]Department of Urology, University Freiburg Medical Center, Freiburg, Germany
[3]German Cancer Consortium (DKTK), Partner site Frankfurt, Germany
[4]German Cancer Research Center (DKFZ), Heidelberg, Germany

Lysine-specific demethylase 1 (LSD1), a histone lysine demethylase with the main specificity for H3K4me2, has been shown to be overexpressed in rhabdomyosarcoma (RMS) tumor samples. However, its role in RMS biology is not yet well understood. Here, we identified a new role of LSD1 in regulating adhesion of RMS cells. Genetic knockdown of LSD1 profoundly suppressed clonogenic growth in a panel of RMS cell lines, whereas LSD1 proved to be largely dispensable for regulating cell death and short-term survival. Combined RNA and ChIP-sequencing performed to analyze RNA expression and histone methylation at promoter regions revealed a gene set enrichment for adhesion-associated terms upon LSD1 knockdown. Consistently, LSD1 knockdown significantly reduced adhesion to untreated surfaces. Importantly, precoating of the plates with the adhesives collagen I or fibronectin rescued this reduced adhesion of LSD1 knockdown cells back to levels of control cells. Using KEGG pathway analysis, we identified 17 differentially expressed genes (DEGs) in LSD1 knockdown cells related to adhesion processes, which were validated by qRT-PCR. Combining RNA and ChIP-sequencing results revealed that, within this set of genes, *SPP1*, *C3AR1*, *ITGA10* and *SERPINE1* also exhibited increased H3K4me2 levels at their promoter regions in LSD1 knockdown compared to control cells. Indeed, LSD1 ChIP experiments confirmed enrichment of LSD1 at their promoter regions, suggesting a direct transcriptional regulation by LSD1. By identifying a new role of LSD1 in the modulation of cell adhesion and clonogenic growth of RMS cells, these findings highlight the importance of LSD1 in RMS.

Introduction

RMS is a soft-tissue sarcoma with a high prevalence in children. It is divided into the two main subgroups of embryonal (eRMS) and alveolar (aRMS) RMS, which differ in their histological presentation as well as their genetic aberrations.[1–4] RMS is commonly treated with a combination of surgery, radiation and combined chemotherapy, which has continually been improved and optimized over the last decades; however, advanced diseases still face poor prognosis.[5,6] Several targeted approaches have been proposed by *in vitro* studies (reviewed in Ref. 7), offering new treatment perspectives. However, the understanding of the molecular biology of this tumor entity remains poorly investigated, making it difficult to identify promising new drug targets.

LSD1, encoded by the gene *KDM1A*, is a histone-lysine demethylase for H3K4me2 and, depending on the cellular context, also for H3K9me2, demethylating the lysine residues into their monomethylated and nonmethylated forms.[8] Since H3K4 and H3K9 methylation have different effects on transcriptional activity, LSD1 can have different functions, which are directed by the complexes to which it is bound.[9] Most commonly, LSD1 is found to be associated with the CoREST complex and exhibits specificity for H3K4me2 causing transcriptional silencing.[10]

Based on its complex role in driving transcriptional activity, LSD1 can influence many cellular processes, which seem to differ in different tissue types. For several carcinomas, it is described

Additional Supporting Information may be found in the online version of this article.

Key words: LSD1, rhabdomyosarcoma, cancer

Abbreviations: aRMS: alveolar RMS; BSA: bovine serum albumin; DEGs: differentially expressed genes; ECM: extracellular matrix; EMT: epithelial-to-mesenchymal transition; ER: endoplasmatic reticulum; eRMS: embryonal RMS; FCS: fetal calf serum; GO: gene ontology; LSD1: lysine-specific demethylase 1; PAI-1: plasminogen activator inhibitor 1; PBS: phosphate-buffered saline; PI: propidium iodide; RMS: rhabdomyosarcoma; SDS: sodium dodecylsulfate

Conflict of interest: The authors declare that they do not have any conflict of interest.

DOI: 10.1002/ijc.32806
History: Received 1 Apr 2019; Accepted 24 Oct 2019; Online 19 Dec 2019

Correspondence to: Simone Fulda, E-mail: simone.fulda@kgu.de

What's new?

Rhabdomyosarcoma is a soft-tissue tumor in children with poor outcome in advanced cases. Using various next-generation sequencing methods, the authors identified a novel role of lysine-specific demethylase (LSD1), an epigenetic regulator involved in stem cell maintenance and carcinogenesis, in rhabdomyosarcoma. LSD1 knockdown reduced clonogenic growth and adhesion of tumor cells, while being largely without effect for cell death and short-term survival, underscoring the nuances of LSD1 action in rhabdomyosarcoma biology.

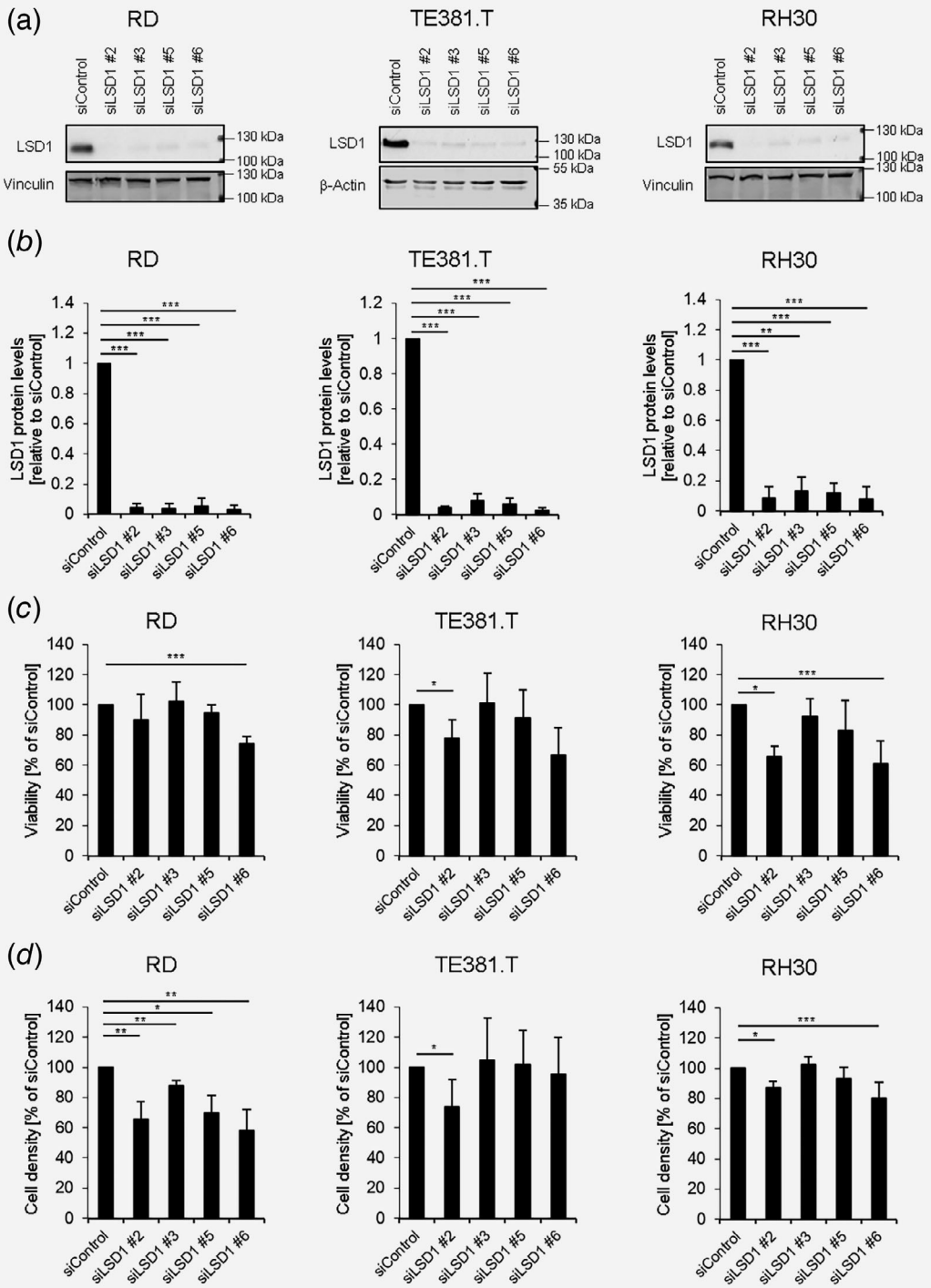

Figure 1. (Continued)

that LSD1 is a main driver of epithelial-to-mesenchymal transition (EMT) and therefore contributes to carcinoma metastasis.[11,12] It is further described that LSD1 plays an important role in stem cell maintenance, implying other tumorigenesis-relevant features.[13–15] In hematological malignancies, LSD1 inhibition has been shown to result in differentiation.[16]

LSD1 has previously been reported to be overexpressed in primary RMS samples and this overexpression is associated with poor prognosis.[17,18] This implicated that LSD1 may represent a potential drug target for RMS treatment. However, specific pharmacological inhibition of LSD1 failed to induce cell death as single agent in RMS cell lines,[19] pointing to a more complex role of LSD1 in RMS biology. So far, LSD1 has not yet been related to any tumorigenic process in RMS, despite its reported high expression levels.

Here, we applied next-generation sequencing approaches to identify and characterize hitherto unknown roles of LSD1 in RMS.

Materials and Methods

Cell culture and chemicals

RD (RRID:CVCL_1649), TE 381.T (RRID:CVCL_1751), TE 671 (RRID:CVCL_1756), Rh18 (RRID:CVCL_1659), Rh36 (RRID:CVCL_M599), TE 441.T (RRID:CVCL_1754) and RMS-13 (RRID:CVCL_UF98) were obtained from the American Type Culture Collection (ATCC; Manassas, VA), Rh30

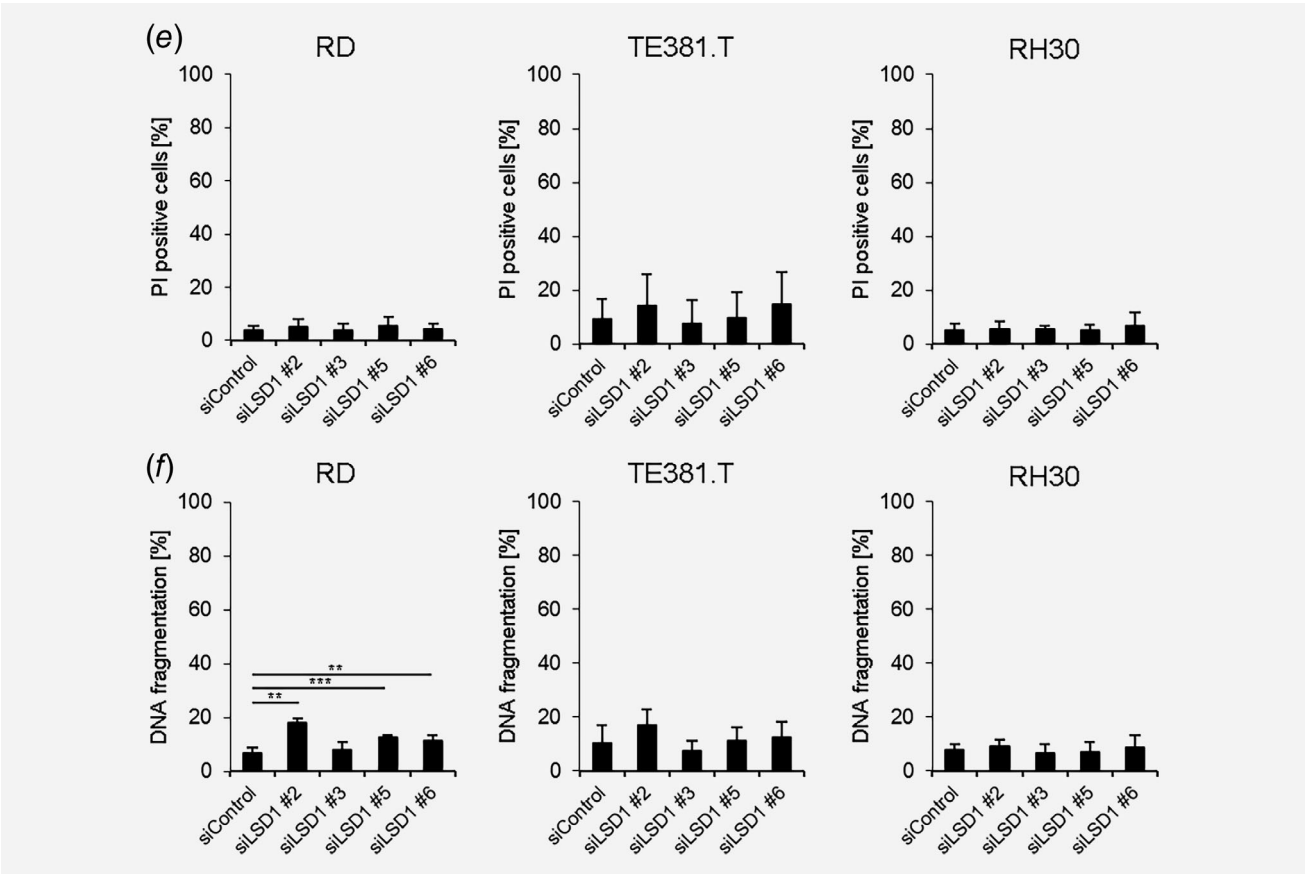

Figure 1. LSD1 is largely dispensable for short-term survival and cell viability of RMS cells. (*a*) RD, TE381.T and RH30 cells were reversely transfected with siRNA against LSD1 mRNA for 96 hr. LSD1 protein levels were detected by Western blotting using Vinculin or β-Actin as loading control. One respective experiment out of three is shown. (*b*) RD, TE381.T and RH30 cells were reversely transfected with siRNA against LSD1 mRNA for 96 hr. LSD1 protein levels were detected by Western blotting using β-Actin as loading control. Western blots were quantified, bands were normalized on β-Actin and are displayed respectively to siControl LSD1 levels. Mean and SD of three independent experiments are shown; ***$p < 0.001$. (*c*) RD, TE381.T and RH30 cells were reversely transfected with siRNA against LSD1 or siControl for 96 hr. Cell viability was measured by MTT assay. Mean and SD of three independent experiments are shown; *$p < 0.05$, ***$p < 0.001$. (*d*) RD, TE381.T and RH30 cells were reversely transfected with siRNA against LSD1 mRNA for 96 hr. Cell density was measured by crystal violet staining followed by photometric measurement of resolved crystal violet. Values are calculated in reference to siControl. Mean and SD of three independent experiments performed in triplicate are shown; *$p < 0.05$, **$p < 0.01$, ***$p < 0.001$. (*e*) RD, TE381.T and RH30 cells were reversely transfected with siRNA against LSD1 mRNA for 96 hr. Cell death was measured by co-staining of Hoechst-33342 and PI using fluorescence microscopy. Mean and SD of three independent experiments performed in triplicate are shown. (*f*) RD, TE381.T and RH30 cells were reversely transfected with siRNA against LSD1 or siControl for 96 hr. Cell death was estimated by measuring DNA fragmentation of PI-stained nuclei using flow cytometry. Mean and SD of three independent experiments are shown; **$p < 0.01$, ***$p < 0.001$.

(RRID:CVCL_0041) and Rh41 (RRID:CVCL_2176) were obtained from the Deutsche Sammlung von Mikroorganismen und Zellkulturen GmbH (DSMZ; Braunschweig, Germany), KYM-1 (RRID:CVCL_3007) were obtained from the Japanese Collection of Research Bioresources Cell Bank (JCRB; Osaka, Japan), the T 174 cells (RRID:CVCL_U955) are of unknown origin, but proved to be authentic by STR Profiling. The TE 671 cells are a derivate of the RD cells, since they originate from the same patient, as well as the Rh30 and the RMS-13 cells derive from the same patient. Cells were maintained in RPMI 1640 or DMEM GlutaMAXX medium (Life Technologies, Inc., Eggenstein, Germany) supplemented with fetal calf serum (FCS), penicillin/streptomycin and sodium pyruvate (Invitrogen, Heidelberg, Germany) as shown in Supporting Information Table S1. All cell lines were authenticated by STR profiling within the last three years and all experiments were performed with mycoplasma-free cells. Chemicals were purchased from Sigma-Aldrich (Taufkirchen, Germany) or Carl Roth (Karlsruhe, Germany) unless otherwise indicated.

siRNA interference

For transient knockdown by siRNA, cells were reversely transfected with SilencerSelect siRNA (Life Technologies) using Lipofectamine RNAiMAX reagent and OptiMEM (both Life Technologies, Inc.). Following siRNA constructs were used: control siRNA (4390842) and targeting siRNAs against LSD1 (s617 (#1); s618 (#2); s619 (#3); s531633 (#5); s531634 (#6)).

Determination of cell viability and cell death

Cell viability was assessed by MTT (3-(4,5-dimethylthiazol-2-yl)-2,5-diphenyltetrazolium bromide) assay according to the manufacturer's instructions (Roche Diagnostics, Mannheim,

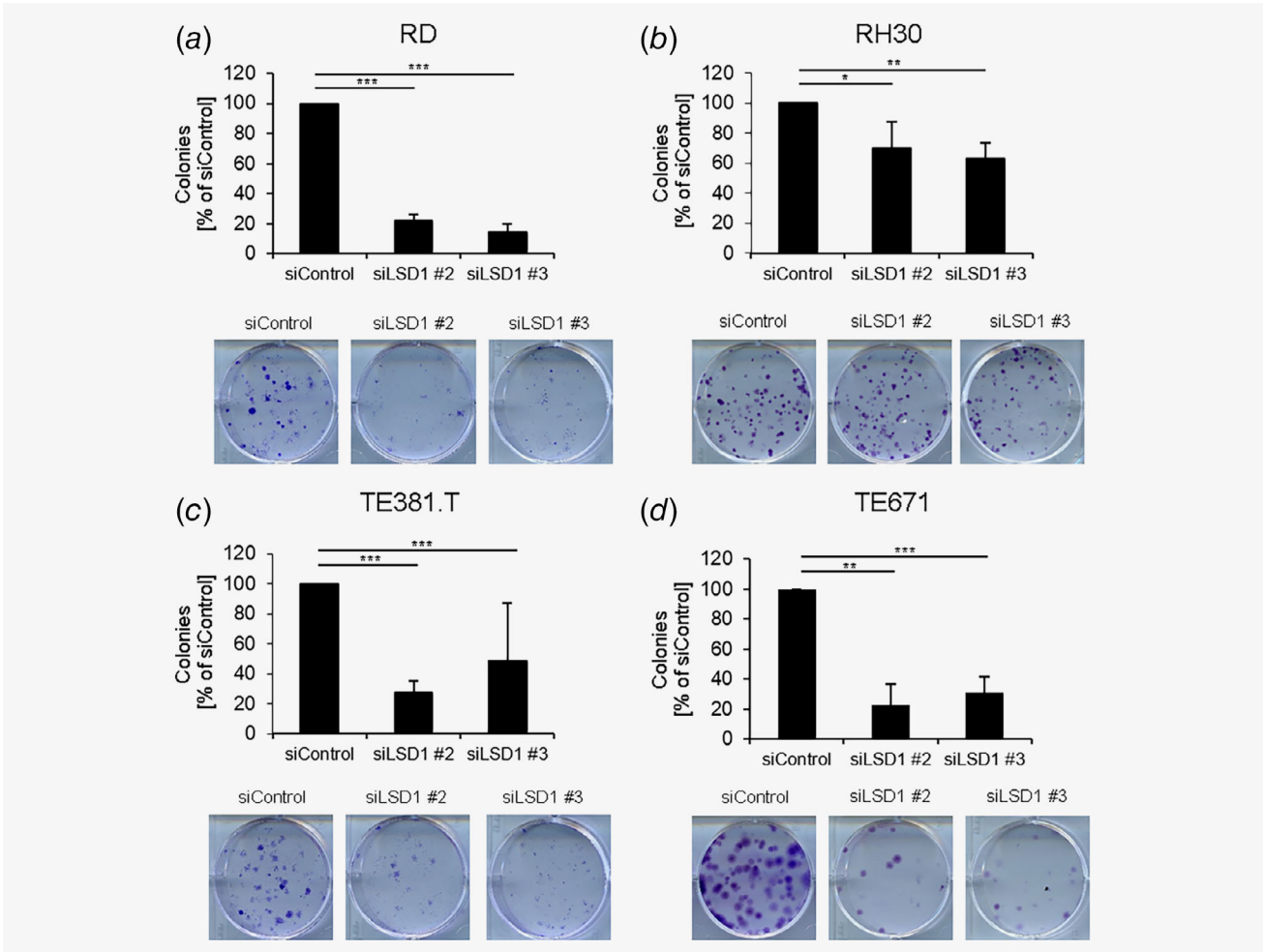

Figure 2. LSD1 knockdown reduces colony formation in a panel of RMS cell lines. RD (*a*), RH30 (*b*), TE381.T (*c*), TE671 (*d*), T174 (*e*), Kym-1 (*f*), RH41 (*g*) and RMS13 (*h*) cells were reversely transfected with siRNA against LSD1 mRNA for 48 hr. LSD1 knockdown cells were seeded at 200 cells per well and colonies were allowed to grow for 10–12 days. Colonies were stained with crystal violet, counted and displayed in reference to siControl (upper panel). A respective well of each condition is shown (lower panel). Mean and SD of three independent experiments performed in triplicate are shown; $*p < 0.05$, $**p < 0.01$, $***p < 0.001$. [Color figure can be viewed at wileyonlinelibrary.com]

Germany). Cell density was measured by staining the cells with crystal violet solution (0.5% crystal violet, 30% ethanol and 3% formaldehyde) and removal of excess stain by washing with tap water. Stained cells were resuspended in 1% sodium dodecylsulfate (SDS) and measured at 550 nm with a photospectrometer. Cell death was measured by flow cytometric analysis (FACS Canto II, BD Biosciences, Heidelberg, Germany) of DNA fragmentation of propidium iodide (PI)-stained nuclei as described before[20] or by fluorescence-based microscope analysis of PI uptake, using Hoechst 33342 and PI double staining (both Sigma-Aldrich) as well as the ImageXpress Micro XLS Widefield High-Content Analysis System and MetaXpress® Software according to the manufacturer's instructions (Molecular Devices, Sunnyvale, CA).

Colony formation assays

For colony formation assays, cells were reversely transfected with siRNA against LSD1 or control siRNA for 48 hr in a 24-well plate. Knockdown cells were trypsinized, counted and reseeded at 200 cells per six-well (9.6 cm^2). Colonies were allowed to grow for 10–12 days and stained with crystal violet solution (0.5% crystal violet, 30% ethanol and 3% formaldehyde) for manual counting of visible colonies.

Western blotting

Western blotting was conducted as described previously[21] using RIPA buffer. For detection the following primary antibodies were used: mouse anti-LSD1 (Novus Biologicals, Littleton, CO, No. NB100-1762), mouse anti-Plasminogen activator inhibitor 1 (PAI-1) (Santa Cruz Biotechnology, Santa Cruz, CA, No. sc-5297), mouse anti-Vinculin (Sigma, No. V9131), mouse anti-β-Actin (Sigma, No. A5441), mouse anti-GAPDH (HyTest, Turku, Finland, No. 5G4-6C5). Goat anti-mouse IgG conjugated to horseradish peroxidase (Santa Cruz Biotechnology, Santa Cruz, CA) or donkey anti-mouse IgG conjugated to horseradish peroxidase (Abcam, Cambridge, UK, No. ab96876) were used as secondary antibodies. Enhanced chemiluminescence (Thermo Fisher, Waltham, MA) or

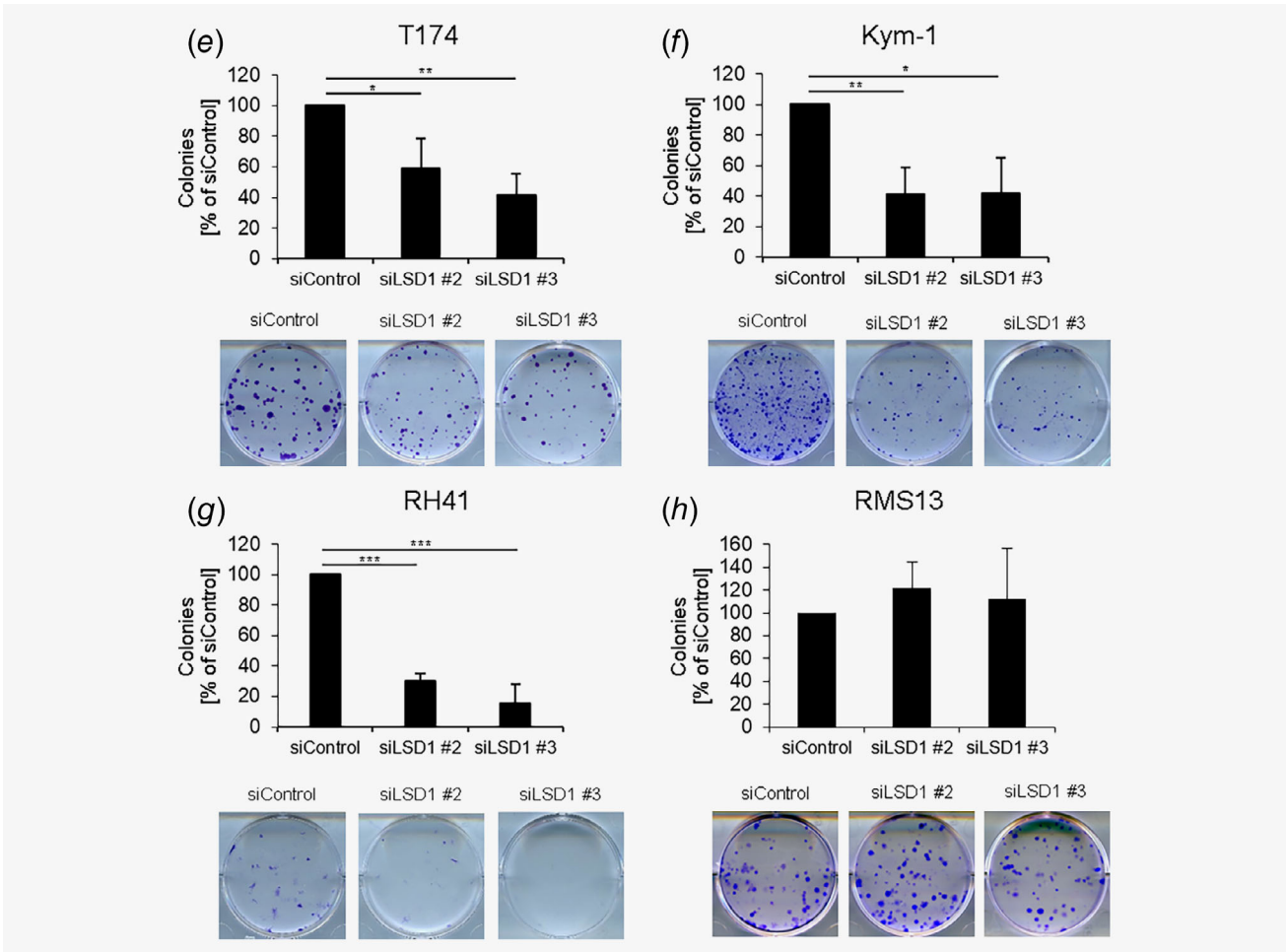

Figure 2. (Continued) [Color figure can be viewed at wileyonlinelibrary.com]

infrared dye-labeled secondary antibodies and infrared imaging (Odyssey Imaging System, LICOR Bioscience, Bad Homburg, Germany) were used for detection. Representative blots of at least two independent experiments are shown. For quantification of Western blots three independent experiments were performed and band intensity was determined by using ImageJ software with normalization of the signal to β-Actin as loading control.

RNA sequencing and quantitative real-time PCR

For analysis of mRNA expression levels, total RNA was isolated by using peqGOLD Total RNA kit (Peqlab, Erlangen, Germany) according to the manufacturer's instructions. For the RNA which was sent for sequencing (DKFZ Genomics and Proteomics Core Facility, Sequencing: paired-end, 100 bp) the additional step for DNA digestion was included. For cDNA-synthesis, 1 µg of total RNA was used to synthesize the corresponding cDNA using the RevertAid H Minus First Strand cDNA Synthesis Kit (MBI Fermentas GmbH, St. Leon-Rot, Germany) according to the manufacturer's protocol with the use of the random primers. For quantification of gene expression levels, SYBR-green-based quantitative real-time PCR (Applied Biosystems, Darmstadt, Germany) was performed using the Quant Studio 7 Flex real-time PCR system (Applied Biosystems) and Quant Studio RealTime PCR software version 1.3. Data were normalized on 28S-rRNA and GAPDH expression as a reference by using the mean Ct value. Analysis of the melting curves served as control for the specificity of the amplified products. Relative expression levels of the target transcripts were calculated compared to the reference mean Ct by using the $\Delta\Delta c_t$ method. Three independent experiments in triplicate were performed for each gene. All primers were purchased by Eurofins (Hamburg, Germany) and are listed in Supporting Information Table S2 for mRNA targets and in Supporting Information Table S3 for genomic promoter regions.

ChIP-sequencing and ChIP qPCR

Cells were fixed with 1% paraformaldehyde in phosphate-buffered saline (PBS) for 20 min and harvested followed by centrifugation. The pellet was resuspended in incubation buffer for 1 hr. For nuclear extracts, cells were lysed manually with a douncer in TSE I ChIP lysis buffer followed by sonication (Covaris M220). DNA content was measured using a Nanodrop1000 (Peqlab, Erlangen, Germany) and the samples were split into 50 µg DNA for input and 250 µg for each sample. To each sample salmon sperm DNA and PIC were added with dilution buffer to achieve equal volumes as well as 5 µg of the respective antibody overnight at 4°C: anti-rabbit H3K4me2 (Diagenode, Liège, Belgium), anti-rabbit LSD1 (ab17721, Abcam, Cambridge, UK), anti-rabbit IgG (ab171870, Abcam, Cambridge, UK). The next day 30 µl of Dynabeads Protein G (Thermo Fisher) was added to the suspension for additional 4 hr. DNA-bead-complexes were washed with TSE I, TSE II and Buffer III each 10 min at 4°C and shortly two times with TE buffer prior to elution. DNA antibody complexes were eluted from the beads with elution buffer for 1 hr at room temperature shaking with 1,400 rpm. Afterwards, beads were removed and crosslink was resolved by incubating the samples at 65°C shaking at 1,400 rpm overnight. Samples were treated with Proteinase K prior to DNA purification with Zymo Kit according to the manufacturer's instructions. DNA was quantitated with the Qubit HS DNA assay and used for sequencing (DKFZ Genomics and Proteomics Core Facility, Sequencing: single end, 50 bp) or qRT-PCR (150 pg/reaction). All buffers are listed in detail in Supporting Information Table S4.

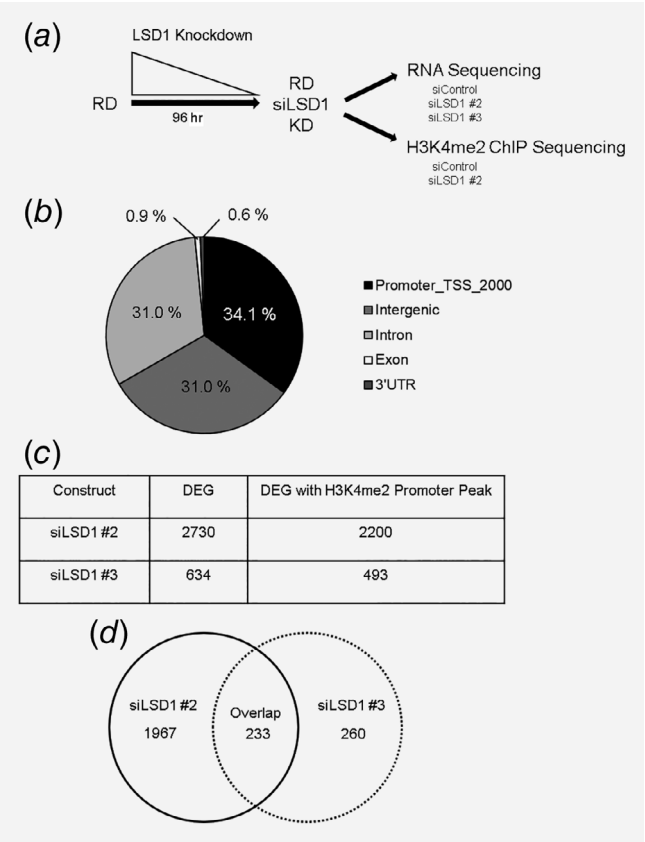

Figure 3. Knockdown of LSD1 leads to deregulation of genes associated with the ECM. (*a*) Schematic view on the experimental set-up for RNA and ChIP-sequencing. (*b*) Analysis of the distribution of the H3K4me2 binding sites in the pooled siControl ChIP. (*c*) DEGs were filtered for significance ($p \leq 0.00001$) and further for H3K4me2 occupancy at their promoter sites in siControl. Remaining genes after the respective filtering are displayed in the table. (*d*) The Venn diagram shows the overlap of DEGs with H3K4me2 peaks at their promoters of siLSD1 construct #2 and #3, in following referred to as the overlap. (*e*) GO analysis Biological Process for the overlap done with EnrichR and sorted for adjusted *p*-value. Top 20 enriched GO terms are displayed. (*f*) KEGG pathways enrichment analysis for the overlap done with EnrichR and sorted for adjusted *p*-value. Enriched pathways with $p_{adj} \leq 0.5$ are shown.

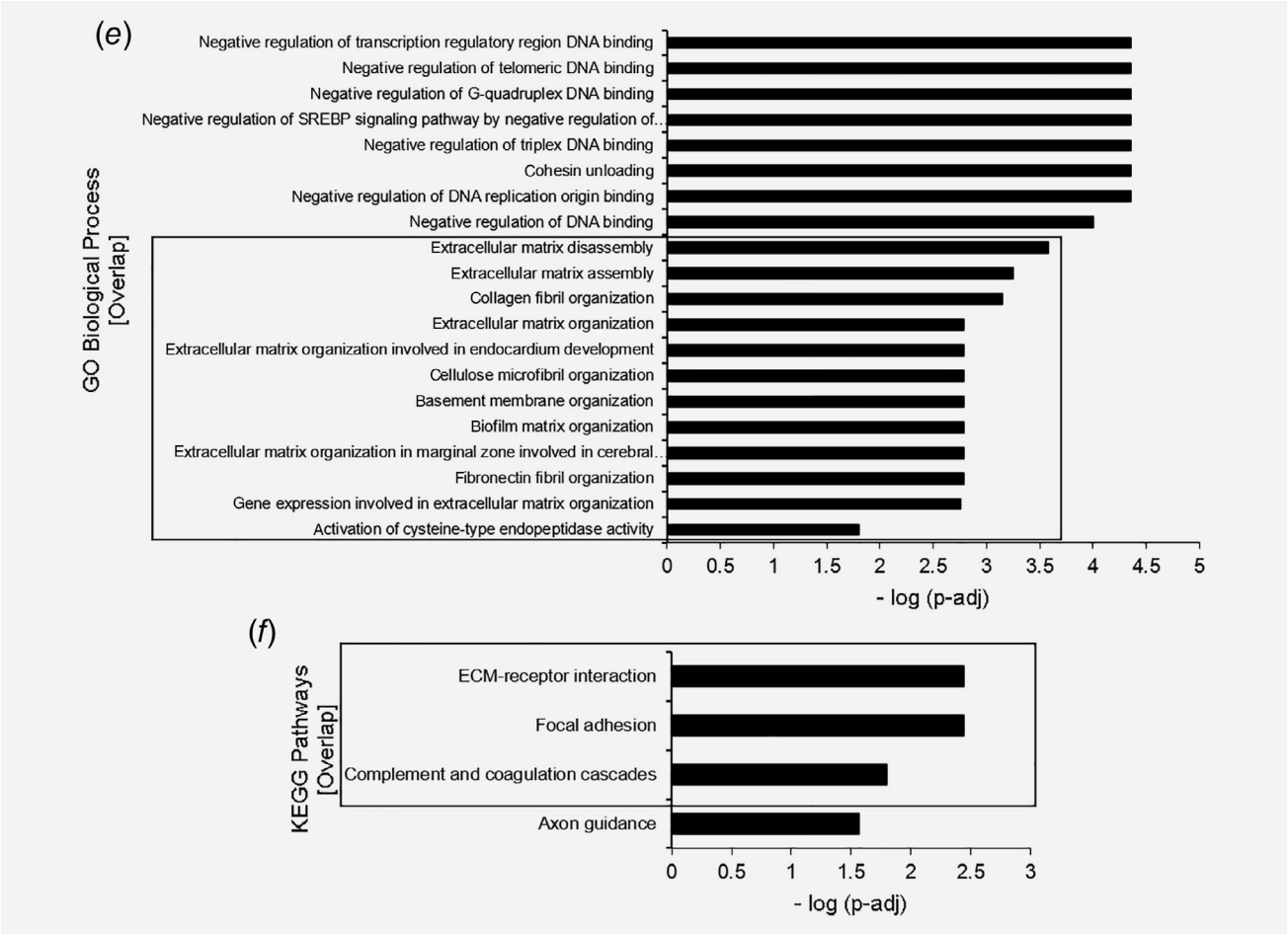

Figure 3. (Continued)

Adhesion assays

Suspension cell culture plates were coated with PBS, collagen I or fibronectin prior to cell seeding. Adhesives were allowed to bind for 1.5 hr, washed twice and blocked with media containing 10% FCS for 30 min at 37°C. Plates were washed again twice and knockdown cells were reseeded at a density of 80,000 cells/cm^2 in serum-free media. Following adhesion for limited time, nonadherent cells were removed and the plate was washed three times with PBS. Adherent cells were stained with crystal violet solution. Excessive stain was washed away with ddH_2O and the plate left for air-drying. Crystal violet was resolved with 1% SDS and measured at 550 nm with a spectrophotometer. CytoSelect Matrix Adhesion Assay (BioCat, Heidelberg, Germany) was used as recommended by the manufacturer with 90,000 cells/cm^2 in serum-free media and 45 min adhesion time.

Data availability

Data available on request from the authors. The sequencing data that support the findings of our study are openly available in the database Gene Expression Omnibus (GEO) under the accession number GSE140041 at https://www.ncbi.nlm.nih.gov/geo/query/acc.cgi?acc=GSE140041.

Additional methods can be found in the Supporting Information.

Results

LSD1 is largely dispensable for short-term survival of RMS cells

Since it has been reported that RMS patient samples exhibit high levels of LSD1, we addressed key parameters of tumor cells after knockdown of LSD1 using embryonal (RD, TE381.T) and alveolar (RH30) RMS cell lines as models. Efficient knockdown of LSD1 using four different siRNA constructs was confirmed in all three cell lines after 96 hr (Figs. 1*a* and 1*b*, Supporting Information Figs. S1*a*–S1*c*). To investigate whether LSD1 affects cell viability, we measured metabolic activity and cell density after LSD1 knockdown. LSD1 knockdown caused a slight to moderate reduction of metabolic activity and cell density in RMS cells (Figs. 1*c* and 1*d*), while it had little effects on cell death as determined by analysis of DNA fragmentation and of PI uptake, a parameter of plasma membrane permeability (Figs. 1*e* and 1*f*).

To explore whether LSD1 knockdown affects cell cycle progression we determined the distribution of RMS cells to the different cell cycle phases. However, LSD1 knockdown did not substantially alter cell cycle progression (Supporting Information Figs. S2*a*–S2*c*). This set of experiments indicates that LSD1 is largely dispensable for short-term survival of RMS cells.

LSD1 knockdown reduces colony formation in a panel of RMS cell lines

Since we found little involvement of LSD1 in the regulation of cell death and cell viability in short-term assays, we next assessed proliferation over a prolonged period of time in a starvation setup. Under these conditions, LSD1 knockdown

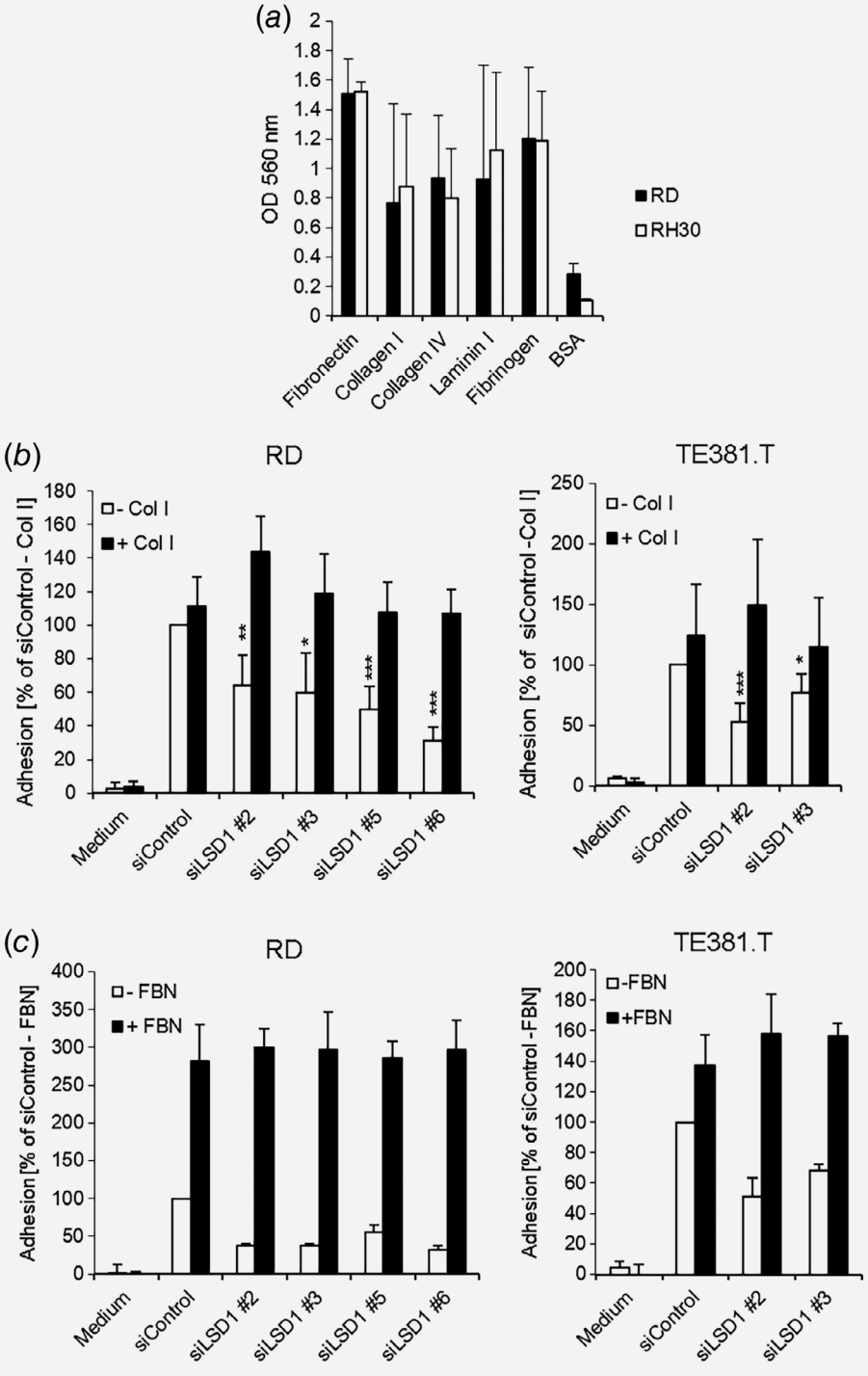

Figure 4. (Continued).

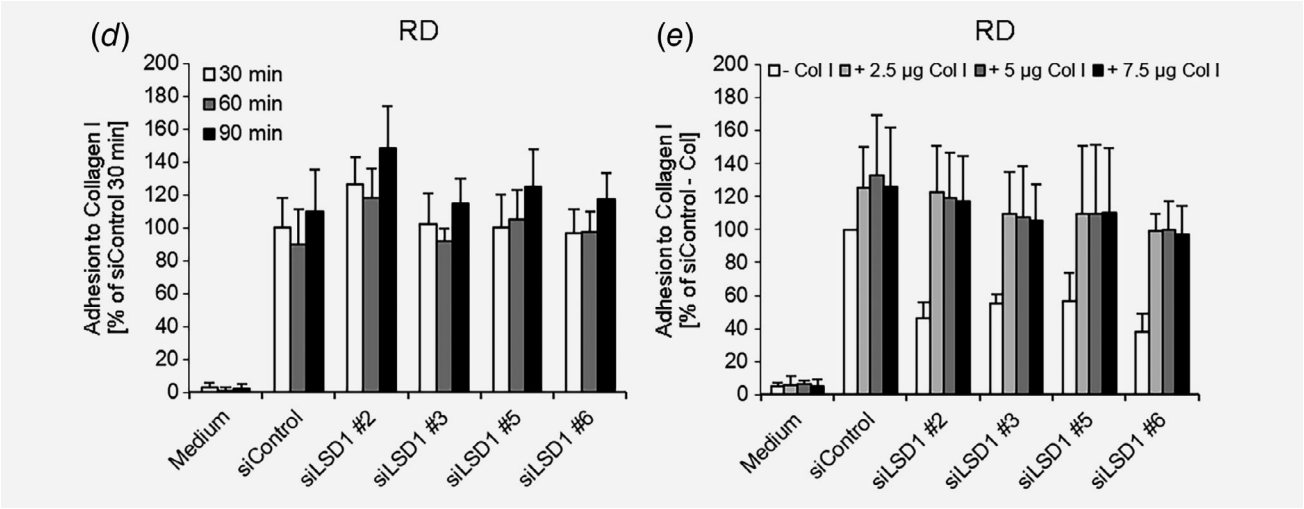

Figure 4. LSD1 knockdown changes the adhesive properties of RMS cells to untreated surfaces. (*a*) RD and RH30 cells were reversely transfected with siRNA against LSD1 or siControl for 96 hr. Cells were detached, counted and seeded for adhesion for 45 min on a Cytoselect Matrix Adhesion Array using colorimetric quantification of adhesion. Mean and SD of three experiments performed as singlets is shown. (*b*) Plates were coated with 5 µg/cm^2 collagen I. RD and TE381.T cells were reversely transfected with siRNA against LSD1 or siControl for 96 hr. Cells were detached, counted and seeded for adhesion for 30 min. Adherent cells were stained with crystal violet after extensive washing, resolved in 1% SDS and quantified with a photospectrometer. Mean and SD of three independent experiments in triplicate are shown. Displayed significance levels were calculated for each construct in comparison to siControl without coating. *$p < 0.05$, **$p < 0.01$, ***$p < 0.001$. (*c*) Plates were coated with 1 µg/cm^2 fibronectin. RD and TE381.T cells were reversely transfected with siRNA against LSD1 or siControl for 96 hr. Cells were detached, counted and seeded for adhesion for 30 min. Adherent cells were stained with crystal violet after extensive washing. Mean and SD of three independent experiments in triplicate are shown. (*d*) Plates were coated with 5 µg/cm^2 collagen I. RD cells were reversely transfected with siRNA against LSD1 or siControl for 96 hr. Cells were detached, counted and seeded for adhesion for 30, 60 and 90 min. Adherent cells were stained with crystal violet after extensive washing. Mean and SD of three independent experiments in triplicate are shown. (*e*) Plates were coated with 2.5, 5 or 7.5 µg/cm^2 collagen I. RD cells were reversely transfected with siRNA against LSD1 or siControl for 96 hr. Cells were detached, counted and seeded for adhesion for 30 min. Adherent cells were stained with crystal violet after extensive washing. Mean and SD of three independent experiments in triplicate are shown.

cells exhibited significantly reduced growth after 144 hr compared to siControl cells (Supporting Information Fig. S2*d*).

Furthermore, we investigated long-term effects of LSD1 knockdown by colony formation assay. Importantly, knockdown of LSD1 resulted in strongly reduced clonogenic growth in RD and TE381.T cells and also significantly reduced colony formation of RH30 cells (Figs. 2*a*–2*c*, Supporting Information Figs. S3*a*–S3*c*). To test the general relevance of this finding we extended these experiments to a panel of RMS cell lines. Of note, LSD1 silencing significantly reduced colony formation also in several additional RMS cell lines (TE671, TE381.T, T174, Kym-1 and RH41) with the exception of RMS13 cells (Figs. 2*d*–2*h*, Supporting Information Figs. S3*d*–S3*h*). Control experiments confirmed that LSD1 expression was knocked down at least up to 144 hr after gene silencing (Supporting Information Figs. S3*j* and S3*k*). These findings show that LSD1 knockdown suppresses colony formation in a panel of RMS cell lines pointing to an effect on long-term growth.

To determine whether LSD1 is differentially expressed in eRMS and aRMS we analyzed basal LSD1 protein levels in a panel of RMS cell lines. However, we did not find any obvious correlation between LSD1 expression and histological subtype of RMS or sensitivity to LSD1 knockdown (Supporting Information Fig. S3*l*).

Since reduced tumor cell growth might be a result of increased differentiation, we assessed expression levels of key markers of myogenic differentiation, namely, MEF2C, Myogenin and MyoD using qRT-PCR. However, LSD1 knockdown did not consistently alter differentiation markers in RD, TE381.T and RH30 cells (Supporting Information Figs. S4*a*–S4*c*).

Knockdown of LSD1 leads to deregulation of genes associated with the extracellular matrix

To gain insights into the functions of LSD1 in RMS we performed RNA sequencing in parallel with ChIP-sequencing using LSD1 knockdown and control RD cells (Fig. 3*a*). RNA sequencing showed that *KDM1A* (LSD1) was the strongest downregulated gene confirming the efficacy of gene silencing (Supporting Information Tables S5 and S6). Since LSD1 is known to induce transcriptional changes predominately via its histone targets, that is, the histone modification H3K4me2,[10] we used ChIP-sequencing for H3K4me2 to further explore promoter modulation upon LSD1 knockdown. Approximately one-third of the detected H3K4me2 peaks in RD control cells associated with promoter

regions (Fig. 3*b*). Analysis of the RNA sequencing results for DEGs upon LSD1 knockdown yielded 2,730 genes for siLSD1 construct #2 and 634 for siLSD1 construct #3 (Fig. 3*c*). To identify genes that are directly regulated by LSD1 we then restricted the DEGs to those which have an H3K4me2 peak at their promoter in siControl cells. This approach revealed 2,200 genes for siLSD1 construct #2 and 493 for siLSD1 construct #3 with H3K4me2 promoter occupancy in siControl cells (Fig. 3*c*). A comparison of the genes filtered for promoter occupancy and the unfiltered number of genes showed that almost all DEGs had an H3K4me2 promoter occupancy and were therefore potential direct targets of LSD1 (Fig. 3*c*). For further analysis of the sequencing data by gene

(*a*)

KEGG Pathway Term	Contributing Genes
ECM-receptor interaction	PROCR, PLAU, SERPINE1, C3AR1, PLAUR, TFPI
Focal adhesion	PDGFRB, COL2A1, ITGA10, COL9A1, SPP1, ITGB8, FLNC, ITGA5, THBS2, MET, MYLK
Complement and coagulation cascades	COL2A1, ITGA10, COL9A1, SPP1, ITGB8, ITGA5, THBS2

(*b*)

Gene	Protein	siLSD1 #2		siLSD1 #3	
		log2 Fold Change	p-Value	log2 Fold Change	p-Value
SERPINE1	serpin family E member 1	3.56	5.53E-61	0.83	6.81E-07
C3AR1	complement C3a receptor 1	3.51	4.51E-50	3.14	5.27E-32
PLAUR	plasminogen activator, urokinase receptor	2.25	2.24E-57	0.94	2.76E-13
ITGA10	integrin subunit alpha 10	1.8	6.39E-13	1.43	1.43E-09
MET	MET proto-oncogene, receptor tyrosine kinase	1.76	2.81E-26	1.15	1.40E-05
PLAU	plasminogen activator, urokinase	1.7	3.24E-46	0.93	1.51E-08
PDGFRB	platelet derived growth factor receptor beta	1.53	7.12E-22	0.82	5.30E-07
SPP1	secreted phosphoprotein 1	1.44	8.86E-26	0.55	1.40E-05
ITGB8	integrin subunit beta 8	1.44	3.92E-21	1.15	7.18E-05
PROCR	protein C receptor	1.36	2.56E-24	0.68	9.95E-05
ITGA5	integrin subunit alpha 5	1.18	1.74E-16	0.62	4.51E-07
THBS2	thrombospondin 2	0.86	1.28E-15	0.54	2.34E-04
MYLK	myosin light chain kinase	0.52	1.87E-05	0.74	4.48E-09
TFPI	tissue factor pathway inhibitor	0.51	9.70E-08	0.5	1.59E-04
FLNC	filamin C	-0.73	7.77E-12	-0.6	2.59E-05
COL9A1	collagen type IX alpha 1 chain	-0.96	8.86E-05	-1.3	2.17E-06
COL2A1	collagen type II alpha 1 chain	-1.05	2.65E-10	-1.61	8.72E-17

Figure 5. LSD1 binds to promoters of DEGs involved in ECM modulation. (*a*) Listing of genes contributing to the enrichment of the KEGG pathways (Fig. 3*f*). (*b*) Detailed list of the 17 genes from (*a*) with the annotations, log2 fold change and adjusted *p*-value for siLSD1 constructs #2 and #3, showing 14 upregulated and three downregulated genes. The list is sorted by descending log2 fold change of siLSD1 #2. (*c*) Visualization of H3K4me2 peaks in siControl and siLSD1 at the promoter regions (+2000 bp and −2000 bp of the TSS) of SPP1, C3AR1, ITGA10 and SERPINE1. The tracks are shown separately and as overlay (siControl in black, siLSD1 in light gray). Furthermore, the localization of the counted peaks is shown below together with the TSS RefSeq annotation for the gene. The remaining 14 genes are shown in Supporting Information Fig. S7. (*d*) Validation of differential regulation by siLSD1 knockdown in the RNA sequencing with qRT-PCR for the genes SPP1, C3AR1, ITGA10 and SERPINE1. For this, RD and TE381.T cells were reversely transfected with siRNA against LSD1 or siControl for 96 hr. GAPDH and 28S-rRNA were used as a reference and for normalization. Values are displayed relative to siControl. Mean and SD of three independent experiments in triplicate are shown. *$p < 0.05$, **$p < 0.01$, ***$p < 0.001$. (*e*) RD and TE381.T cells were reversely transfected with siLSD1 #2, siLSD1 #5, silSD1 #6 or siControl for 96 hr. PAI-1 and LSD1 protein levels were detected by Western blotting using GAPDH as loading control. One respective experiment out of three is shown. (*f*) RD cells were reversely transfected with siControl and siLSD1 #2 for 96 hr. ChIP protocol was applied for precipitation of LSD1 and the DNA was used for qRT-PCR with genomic primers for the targets SPP1, SERPINE1, ITGA10 and C3AR1. For the specificity of the LSD1-ChIP results, we used siLSD1 cells.

ontology (GO) and pathway enrichment, we focused on the overlap of the previously filtered genes of siLSD1 construct #2 and construct #3 (Fig. 3*d*). Interestingly, we found an enrichment for GO terms (GO: Biological Process) with extracellular matrix (ECM) association, ECM signaling and focal adhesion in the pathway analysis using the KEGG database (Figs. 3*e* and 3*f*). In addition, GO terms for the cellular compartment showed a strong enrichment for endoplasmatic reticulum (ER) compartments (Supporting Information Fig. S5*a*), which enriched in particular due to several collagens and other secreted ECM proteins (Supporting Information Fig. S5*b*), indicating an association with the ECM rather than a direct effect on the ER itself.

LSD1 knockdown changes adhesive properties of RMS cells to untreated surfaces

Since our analysis by GO and pathway enrichment pointed to LSD1-mediated regulation of ECM and adhesion, we next investigated if LSD1 silencing affects adhesive properties of RMS cells using adhesion assays with different surface coatings. Since little is yet known about the adhesive properties of RMS cells, we initially used a Cytoselect Matrix Adhesion Array to test basal binding abilities. This screening revealed that RD and RH30 cells were able to adhere to several ECM components and in particular to fibronectin, whereas only the adhesion to bovine serum albumin (BSA)-coated surfaces was

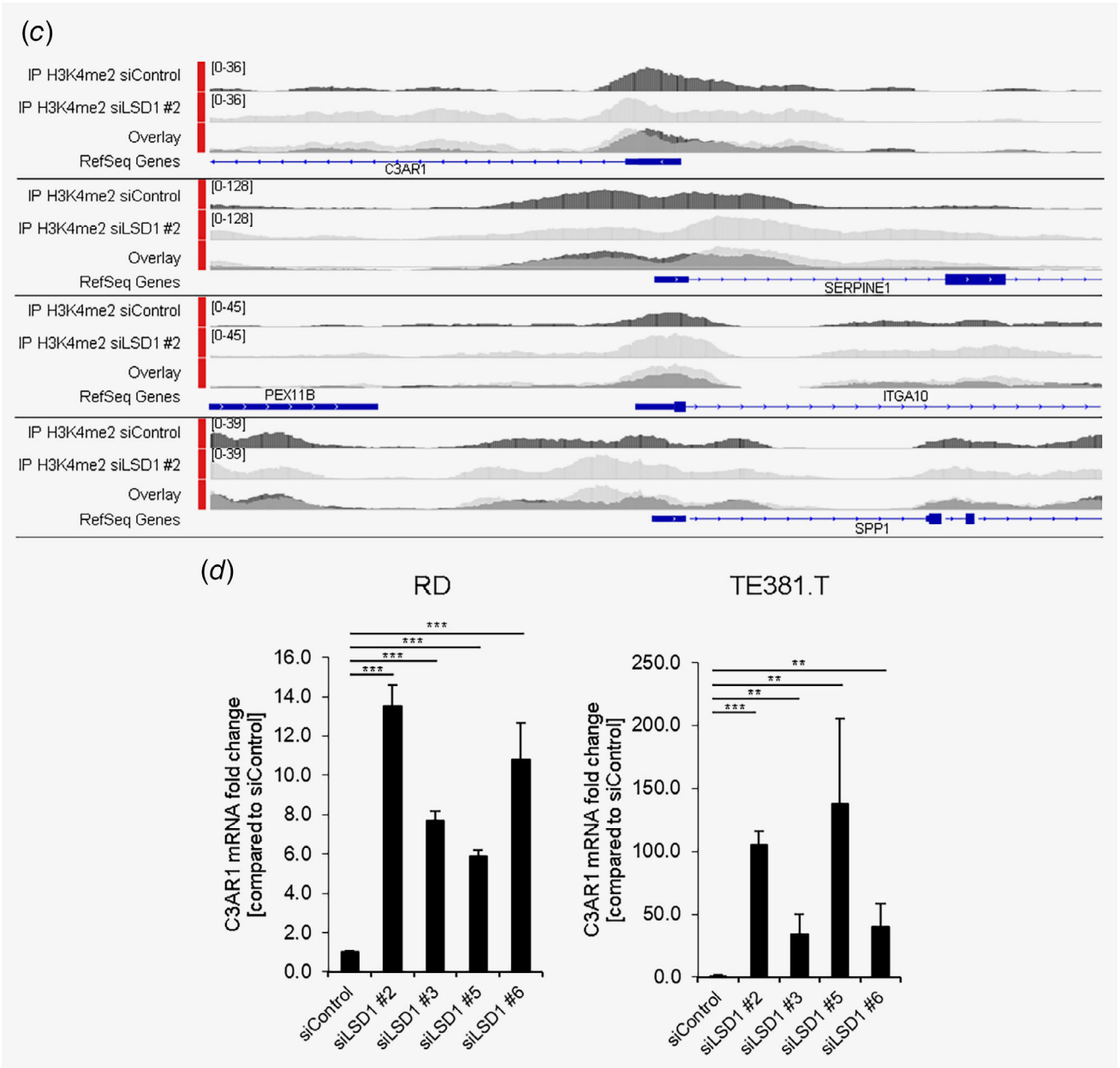

Figure 5. (Continued). [Color figure can be viewed at wileyonlinelibrary.com]

very low (Fig. 4*a*). To investigate whether LSD1 regulates adhesive properties of RMS cells we compared the ability of LSD1 knockdown and control RMS cells to adhere to non-tissue culture-treated polystyrene cell culture plates in the presence and absence of collagen I or fibronectin. Interestingly, LSD1 knockdown significantly impaired the ability of RD and TE381.T cells to adhere to the plate compared to control cells (Figs. 4*b* and 4*c*). Intriguingly, this phenotype upon LSD1 knockdown was completely rescued by the application of collagen I, resulting in a comparable adhesion pattern of LSD1 knockdown and control cells in the presence of collagen I (Fig. 4*b*). Similarly, application of fibronectin completely restored the ability of LSD1 knockdown RD and TE381.T cells to adhere to the plate (Fig. 4*c*). By comparison, constitutive adherence of RH30 cells to the plate alone was very low and did not significantly differ between LSD1 knockdown and control cells (Supporting Information Figs. S6*a* and S6*b*). Also, RH30 cells did strongly adhere to both, collagen I and fibronectin, but without significant differences between LSD1 knockdown and control cells (Supporting Information Figs. S6*a* and S6*b*).

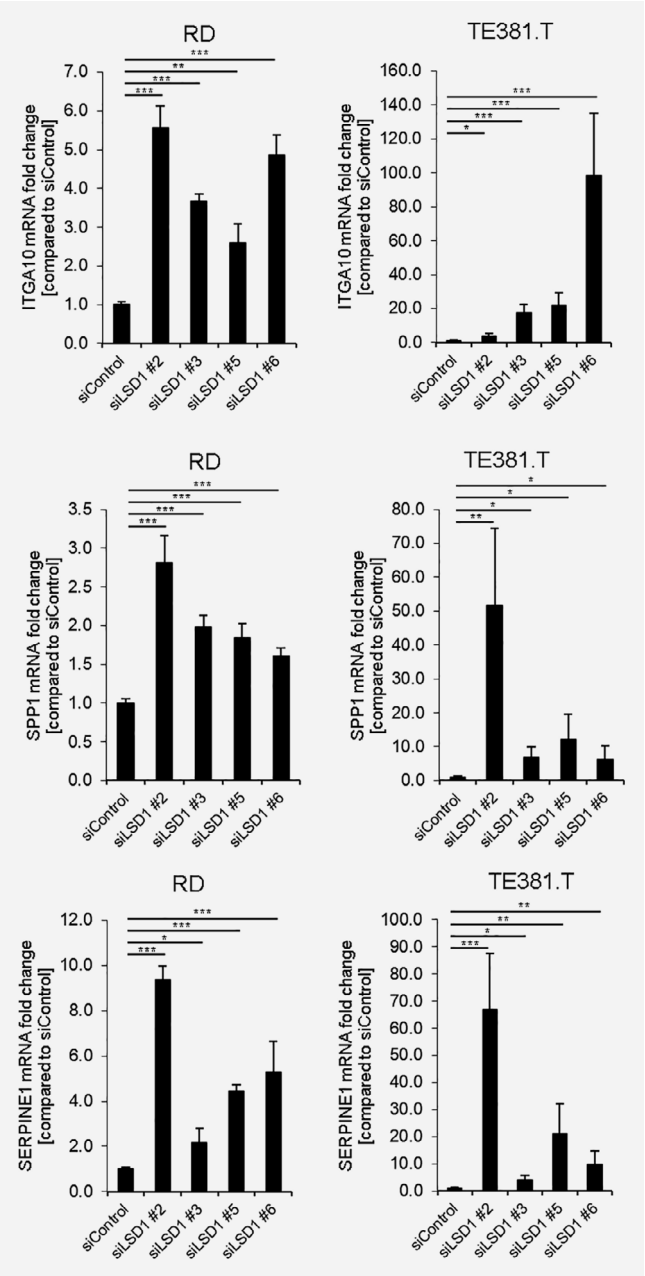

Figure 5. (Continued).

Kinetic experiments measuring the adherence of RD cells to collagen I after 30, 60 and 90 min did not show increased binding after longer adhesion times (Fig. 4*d*). Also, dose-response experiments using various collagen I concentrations to test if the stiffness of the matrix affects adhesion revealed no difference in the range of 2.5–7.5 μg/cm^2 collagen I in RD control and knockdown cells (Fig. 4*e*). Taken together, knockdown of LSD1 affects the binding properties of RD and TE381.T cells to untreated surfaces, which can be restored by the application of ECM proteins such as collagen I or fibronectin. This phenotype is consistent with the results obtained by GO and KEGG pathway enrichment showing a strong association of DEGs with terms related to adhesion.

To explore whether changes in adhesion have an effect on invasion and/or migration of RMS cells we analyzed these parameters upon LSD1 knockdown in RD cells. Using matrigel-coated transwell assay, we found no changes in invasion upon LSD1 knockdown in RD cells (Supporting Information Fig. S6*c*). By comparison, LSD1 knockdown significantly impaired wound closure compared to siControl (Supporting Information Fig. S6*d*).

LSD1 binds to promoters of DEGs involved in ECM modulation

Next, we were interested in DEGs by LSD1 silencing which might be involved in the adhesion phenotype. We therefore investigated the genes contributing to the enrichment of the KEGG pathway terms "ECM receptor interaction", "Focal adhesion" and "Complement and coagulation cascades" upon LSD1 knockdown by two distinct constructs (Fig. 5*a*). Using this approach, we identified 17 upregulated genes including extracellular (secreted) proteins (SPP1, PLAU, SERPINE1, THBS2, TFPI), membrane receptors (MET, PLAUR, C3AR1, PDGFRB) and adhesion-mediating proteins (ITGA10, ITGB8, ITGA5; Fig. 5*b*). Furthermore, the cytoskeleton protein FLNC, as well as the ECM structure proteins COL9A1 and COL2A1, were downregulated upon LSD1 silencing (Fig. 5*b*). A comparison of the counts for these genes showed a stable expression for all 17 possible target genes, with *C3AR1* with the weakest and *FLNC* with the strongest expression. In carcinoma cell lines, LSD1 was shown to silence CHD1 expression going along with induction of EMT. However, in the RD cell line used for our experiments, no *CHD1* expression was detectable (Supporting

Information Fig. S7*a*). To explore if these 17 genes are possible LSD1 target genes we overlaid the H3K4me2 distribution at the promoter regions of LSD1 knockdown and control cells. Interestingly, we found an increase in H3K4me2 and a broadening of the peaks, mostly towards the gene body, for *SPP1*, *C3AR1*, *ITGA10* and *SERPINE1* in LSD1 knockdown cells as compared to control cells (Fig. 5*c*), suggesting a direct LSD1 regulation at the promoter. Validation of these changes in gene expression by qRT-PCR confirmed upregulation of *SPP1*, *C3AR1*, *ITGA10* and *SERPINE1* in RD as well as in TE381.T cells upon LSD1 knockdown (Fig. 5*d*). To test if changes in mRNA expression translate into changes of the respective protein we assessed protein expression of PAI-1, the protein encoded by the gene *SERPINE1*. Of note, LSD1 knockdown caused a strong increase in PAI-1 protein levels compared to siControl in RD and TE381.T cells (Fig. 5*e*), consistent with the increase in *SERPINE1* mRNA levels observed upon LSD1 silencing (Fig. 5*d*). Similarly, validation by qRT-PCR confirmed LSD1 knockdown-dependent upregulation of *PDGFRB*, *ITGA5*, *ITGB8*, *PLAU*, *PLAUR* and *MET* (Supporting Information Figs. S7*b*–S7*g*). As the H3K4me2 peaks at the promoters of these genes remained unchanged or decreased upon LSD1 knockdown (Supporting Information Fig. S8), a direct regulation seems rather unlikely. However, genes that are not differentially regulated by LSD1 knockdown did also not show any changes in the H3K4me2 distribution levels as shown for *MFAP1* and *STYXL1* (Supporting Information Fig. S8, last two tracks). Validation of downregulated genes by qRT-PCR showed consistently decreased mRNA levels upon LSD1 knockdown for *COL9A1* and *COL2A1*, but not for *FLNC* (Supporting Information Figs. S7*h*–S7*k*). Furthermore, H3K4me2 peaks at the promoter regions of *COL2A1* and *FLNC* remained unchanged and decreased at the promoter region of *COL9A1* (Supporting Information Fig. S8).

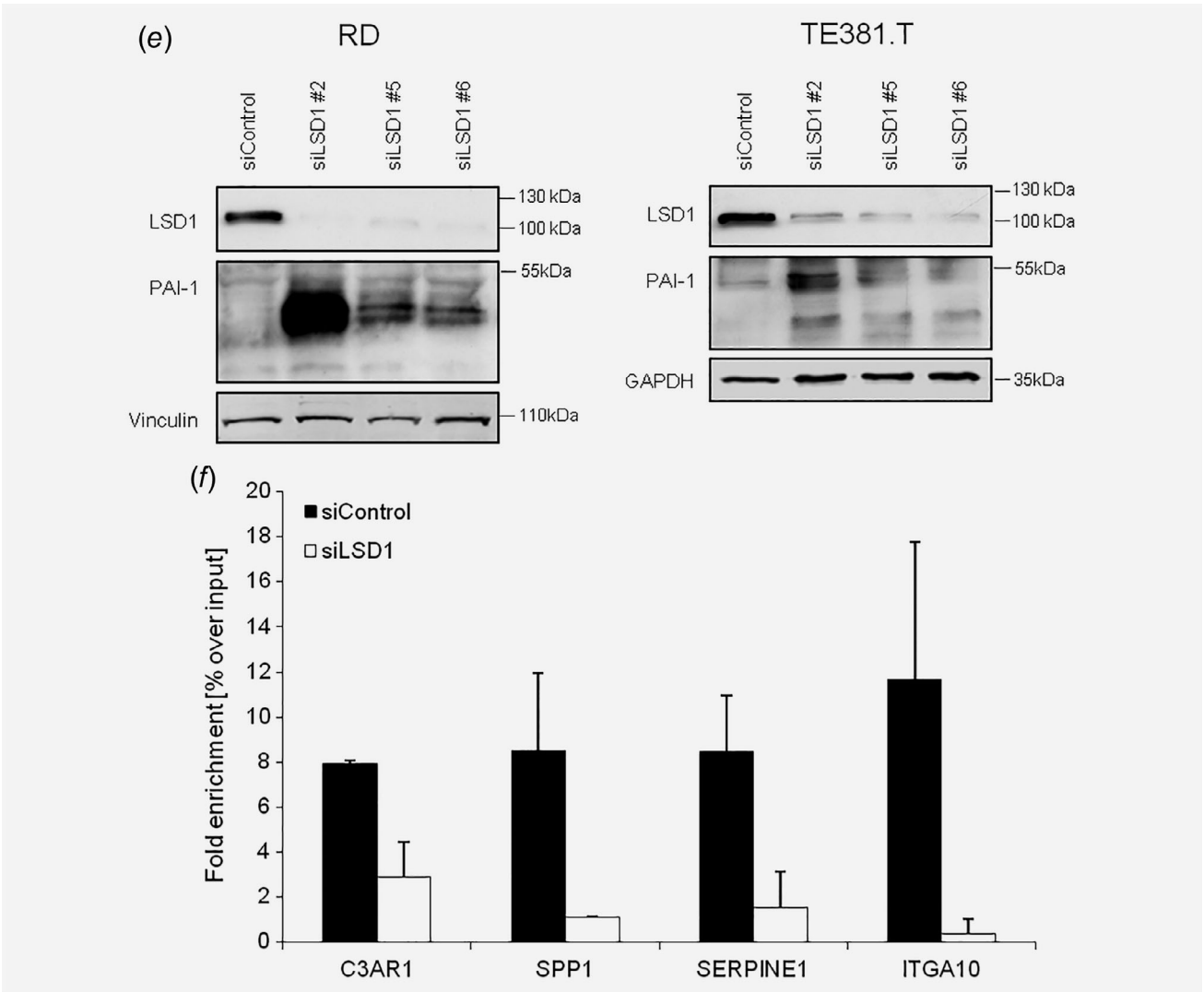

Figure 5. (Continued).

Finally, we investigated if LSD1 directly binds to the promoter regions of the identified and validated candidate genes. To this end, we performed ChIP-qRT-PCR of LSD1 in siControl cells, as an association of LSD1 to the promoter is required for LSD1-dependent direct transcriptional regulation. Of note, *SPP1*, *C3AR1*, *ITGA10* and *SERPINE1* showed an enrichment over input levels for LSD1 at their promoter regions (Fig. 5*f*), indicating that LSD1 is indeed bound to their promoter regions. ChIP-qRT-PCR experiments in siLSD1 cells exhibited a strong reduction in LSD1 promoter-binding upon LSD1 knockdown which confirmed the specificity of the detected enrichment (Fig. 5*f*). Taken together, LSD1 transcriptionally regulates *SPP1*, *C3AR1*, *ITGA10* and *SERPINE1*, which are ECM signaling- and adhesion-associated proteins. This LSD1-dependent transcriptional regulation likely occurs in a direct manner, since LSD1 directly associates with the promoters of these genes.

Discussion

LSD1 has been reported to be highly expressed in RMS patient samples and correlated with highly malignant phenotypes.[18] However, little is so far known on how LSD1 regulates the biology of RMS. Using an exploratory approach of combined RNA and ChIP-sequencing upon LSD1 knockdown coupled with functional analysis, we discovered a new role of LSD1 in the regulation of adhesion in RMS cells.

Our next-generation sequencing approach revealed a putative role of LSD1 in adhesion and ECM signaling. Since LSD1 has been described as a key mediator of EMT,[22–24] it might well contribute to adhesion as part of the change toward a migratory phenotype. So far, the role of LSD1 during EMT has been shown in carcinomas via regulation of E-cadherin expression.[11,22–25] Since RMS are of mesenchymal origin and usually lack E-cadherin expression, the underlying molecular mechanisms responsible for LSD1-dependent regulation of adhesion in RMS likely differ from the mechanisms identified in carcinomas.[26,27] This notion is further underlined by our sequencing data that showed neither any LSD1-dependent regulation of EMT nor E-cadherin expression in RMS cells. Investigation of invasion and wound healing in RD cells revealed decreased wound healing upon LSD1 knockdown but no effects on invasion. The mechanisms underlying the LSD1 contribution to wound healing in mesenchymal RMS cells are another interesting observation besides the adhesion phenotype, which need a more detailed investigation in a broader panel of RMS cell lines.

Our data showing a complete rescue of the defective adhesion phenotype of LSD1 knockdown cells by coating the plates with the adhesives collagen I or fibronectin might give some insights into the mechanisms through which LSD1 might interfere with adhesion. There is the possibility of a dysregulation of the ECM structure.[28] This hypothesis is in line with the common upregulation of *PLAU*, *PLAUR* and *SERPINE1* in LSD1 knockdown cells which all belong to the urokinase system. The urokinase system regulates ECM structure and signaling and has been implicated in the modulation of the tumor environment.[29–31] On the other side, there is also the possibility of a secretory phenotype in which LSD1 knockdown cells are no longer able to secrete the proper ECM they need to attach. This hypothesis is supported by the downregulation of several collagens observed upon LSD1 knockdown. Furthermore, there might well be a link between the signaling events controlling adhesion and clonogenic growth. As the extracellular environment also involves cellular crosstalk, the low-density conditions in the colony assays might further influence the adhesive behavior, leading to less adherent cells upon LSD1 knockdown and therefore fewer colonies. RMS cells are able to build colonies, but little is yet known about the clonogenic potential of RMS cells and the mechanisms regulating these processes. It has been shown for neuroblastoma cells that low-density conditions can influence the growth potential[32] and this might well apply also to the clonogenic growth potential of RMS cells.

An involvement of cell death events in adhesion and clonogenic growth of LSD1 knockdown cells appears rather unlikely, since neither LSD1 knockdown nor pharmacological LSD1 inhibitors, as previously shown,[19] affected cell death in RMS cells, in line with reports on other solid tumors.[33–36] Some of the experiments indicated a dependence of the response to the LSD1 knockdown with the subtype of the RMS cell line, but our analysis of LSD1 protein expression in the different cell lines did not reveal any correlation between LSD1 expression levels and histological subtype. Since the RMS cell lines used in the experiments have various cytogenetic backgrounds, these might well be responsible for different responses to the LSD1 knockdown.

We also consider the involvement of myogenic differentiation as an unlikely cause for the phenotype of defective adhesion and clonogenic growth in LSD1 knockdown cells. The modulation of the epigenetic landscape in RMS has been shown to induce terminal differentiation[37] and LSD1 itself has been found to take part in the regulation of key myogenic differentiation factors, such as MEF2D, MEF2C and MyoD, either by regulating transcription of these factors or by direct protein methylation.[38–40] Differentiation of RMS cells after LSD1 knockdown might explain the reduced clonogenic capacity, since it is known that terminal differentiation goes along with the loss of self-renewal ability. However, our sequencing data and the analysis of expression levels of key myogenic genes do not suggest an increased myogenic differentiation upon LSD1 knockdown. Also, LSD1 was mostly implicated as a driving factor for myogenic differentiation.[38–40] To further elucidate the underlying mechanisms additional studies are required to investigate the link between adhesion and clonogenic growth in LSD1 knockdown RMS cells.

Taken together, we reveal a previously unknown role of LSD1 in adhesion of RMS cells, which might in part be mediated via direct transcriptional regulation of target genes. Given the role of LSD1 in supporting long-term clonogenic survival, LSD1 also turned out to be a relevant therapeutic target in RMS.

Acknowledgements

This work has been partially supported by grants from the BMBF (to S.F.). We thank C. Hugenberg for expert secretarial assistance. We thank the DKFZ Genomics and Proteomics Core Facility (DKFZ, Heidelberg, Germany) for excellent next-generation sequencing services.

References

1. Yang L, Takimoto T, Fujimoto J. Prognostic model for predicting overall survival in children and adolescents with rhabdomyosarcoma. *BMC Cancer* 2014;14:654.
2. Dziuba I, Kurzawa P, Dopierala M, et al. Rhabdomyosarcoma in children—current pathologic and molecular classification. *Pol J Pathol* 2018;69: 20–32.
3. Hayes-Jordan A, Andrassy R. Rhabdomyosarcoma in children. *Curr Opin Pediatr* 2009;21:373–8.
4. Miller RW, Young JL Jr, Novakovic B. Childhood cancer. *Cancer* 1995;75:395–405.
5. Arndt CAS, Bisogno G, Koscielniak E. Fifty years of rhabdomyosarcoma studies on both sides of the pond and lessons learned. *Cancer Treat Rev* 2018;68:94–101.
6. Dantonello TM, Int-Veen C, Harms D, et al. Cooperative trial CWS-91 for localized soft tissue sarcoma in children, adolescents, and young adults. *J Clin Oncol* 2009;27:1446–55.
7. van Erp AEM, Versleijen-Jonkers YMH, van der Graaf WTA, et al. Targeted therapy-based combination treatment in rhabdomyosarcoma. *Mol Cancer Ther* 2018;17:1365–80.
8. Lee MG, Wynder C, Cooch N, et al. An essential role for CoREST in nucleosomal histone 3 lysine 4 demethylation. *Nature* 2005;437:432–5.
9. Metzger E, Wissmann M, Yin N, et al. LSD1 demethylates repressive histone marks to promote androgen-receptor-dependent transcription. *Nature* 2005;437:436–9.
10. Huang PH, Plass C, Chen CS. Effects of histone deacetylase inhibitors on modulating H3K4 methylation Marks - a novel cross-talk mechanism between histone-modifying enzymes. *Mol Cell Pharmacol* 2011;3:39–43.
11. Feng J, Xu G, Liu J, et al. Phosphorylation of LSD1 at Ser112 is crucial for its function in induction of EMT and metastasis in breast cancer. *Breast Cancer Res Treat* 2016;159:443–56.
12. Alsaqer SF, Tashkandi MM, Kartha VK, et al. Inhibition of LSD1 epigenetically attenuates oral cancer growth and metastasis. *Oncotarget* 2017;8: 73372–86.
13. Zhang X, Lu F, Wang J, et al. Pluripotent stem cell protein Sox2 confers sensitivity to LSD1 inhibition in cancer cells. *Cell Rep* 2013;5:445–57.
14. Adamo A, Sese B, Boue S, et al. LSD1 regulates the balance between self-renewal and differentiation in human embryonic stem cells. *Nat Cell Biol* 2011;13:652–9.
15. Yin F, Lan R, Zhang X, et al. LSD1 regulates pluripotency of embryonic stem/carcinoma cells through histone deacetylase 1-mediated deacetylation of histone H4 at lysine 16. *Mol Cell Biol* 2014;34:158–79.
16. Schenk T, Chen WC, Gollner S, et al. Inhibition of the LSD1 (KDM1A) demethylase reactivates the all-trans-retinoic acid differentiation pathway in acute myeloid leukemia. *Nat Med* 2012;18: 605–11.
17. Bennani-Baiti IM, Machado I, Llombart-Bosch A, et al. Lysine-specific demethylase 1 (LSD1/KDM1A/AOF2/BHC110) is expressed and is an epigenetic drug target in chondrosarcoma, Ewing's sarcoma, osteosarcoma, and rhabdomyosarcoma. *Hum Pathol* 2012;43: 1300–7.
18. Schildhaus HU, Riegel R, Hartmann W, et al. Lysine-specific demethylase 1 is highly expressed in solitary fibrous tumors, synovial sarcomas, rhabdomyosarcomas, desmoplastic small round cell tumors, and malignant peripheral nerve sheath tumors. *Hum Pathol* 2011;42:1667–75.
19. Haydn T, Metzger E, Schuele R, et al. Concomitant epigenetic targeting of LSD1 and HDAC synergistically induces mitochondrial apoptosis in rhabdomyosarcoma cells. *Cell Death Dis* 2017;8: e2879.
20. Fulda S, Sieverts H, Friesen C, et al. The CD95 (APO-1/Fas) system mediates drug-induced apoptosis in neuroblastoma cells. *Cancer Res* 1997;57: 3823–9.
21. Heinicke U, Haydn T, Kehr S, et al. BCL-2 selective inhibitor ABT-199 primes rhabdomyosarcoma cells to histone deacetylase inhibitor-induced apoptosis. *Oncogene* 2018;37:5325–39.
22. Lin Y, Wu Y, Li J, et al. The SNAG domain of Snail1 functions as a molecular hook for recruiting lysine-specific demethylase 1. *EMBO J* 2010;29:1803–16.
23. Lin T, Ponn A, Hu X, et al. Requirement of the histone demethylase LSD1 in Snai1-mediated transcriptional repression during epithelial-mesenchymal transition. *Oncogene* 2010;29: 4896–904.
24. Ferrari-Amorotti G, Fragliasso V, Esteki R, et al. Inhibiting interactions of lysine demethylase LSD1 with snail/slug blocks cancer cell invasion. *Cancer Res* 2013;73:235–45.
25. Luo H, Shenoy AK, Li X, et al. MOF acetylates the histone demethylase LSD1 to suppress epithelial-to-mesenchymal transition. *Cell Rep* 2016;15:2665–78.
26. Alba-Castellon L, Batlle R, Franci C, et al. Snail1 expression is required for sarcomagenesis. *Neoplasia* 2014;16:413–21.
27. Chen HN, Yuan K, Xie N, et al. PDLIM1 stabilizes the E-cadherin/beta-catenin complex to prevent epithelial-mesenchymal transition and metastatic potential of colorectal cancer cells. *Cancer Res* 2016;76:1122–34.
28. Frantz C, Stewart KM, Weaver VM. The extracellular matrix at a glance. *J Cell Sci* 2010;123: 4195–200.
29. Huang CY, Chang MC, Huang WY, et al. Urokinase-type plasminogen activator resulting from endometrial carcinogenesis enhances tumor invasion and correlates with poor outcome of endometrial carcinoma patients. *Sci Rep* 2015;5:10680.
30. Thurison T, Almholt K, Gardsvoll H, et al. Urokinase receptor cleavage correlates with tumor volume in a transgenic mouse model of breast cancer. *Mol Carcinog* 2016;55:717–31.
31. Yang XW, Gao F, Chen YJ, et al. The clinical study of Urokinase-type plasminogen activator and vascular endothelial growth factor in gastric cancer. *Cell Biochem Biophys* 2015;72:649–52.
32. Vogler M, Giagkousiklidis S, Genze F, et al. Inhibition of clonogenic tumor growth: a novel function of Smac contributing to its antitumor activity. *Oncogene* 2005;24:7190–202.
33. Huang Y, Vasilatos SN, Boric L, et al. Inhibitors of histone demethylation and histone deacetylation cooperate in regulating gene expression and inhibiting growth in human breast cancer cells. *Breast Cancer Res Treat* 2012;131: 777–89.
34. Vasilatos SN, Katz TA, Oesterreich S, et al. Crosstalk between lysine-specific demethylase 1 (LSD1) and histone deacetylases mediates antineoplastic efficacy of HDAC inhibitors in human breast cancer cells. *Carcinogenesis* 2013;34: 1196–207.
35. Singh MM, Johnson B, Venkatarayan A, et al. Preclinical activity of combined HDAC and KDM1A inhibition in glioblastoma. *Neuro Oncol* 2015;17:1463–73.
36. Singh MM, Manton CA, Bhat KP, et al. Inhibition of LSD1 sensitizes glioblastoma cells to histone deacetylase inhibitors. *Neuro Oncol* 2011;13: 894–903.
37. Ciarapica R, Carcarino E, Adesso L, et al. Pharmacological inhibition of EZH2 as a promising differentiation therapy in embryonal RMS. *BMC Cancer* 2014;14:139.
38. Choi J, Jang H, Kim H, et al. Histone demethylase LSD1 is required to induce skeletal muscle differentiation by regulating myogenic factors. *Biochem Biophys Res Commun* 2010;401:327–32.
39. Choi J, Jang H, Kim H, et al. Modulation of lysine methylation in myocyte enhancer factor 2 during skeletal muscle cell differentiation. *Nucleic Acids Res* 2014;42:224–34.
40. Scionti I, Hayashi S, Mouradian S, et al. LSD1 controls timely MyoD expression via MyoD Core enhancer transcription. *Cell Rep* 2017;18: 1996–2006.